Received 25 October 2024; revised 27 November 2024; accepted 18 December 2024. Date of publication 23 December 2024;
date of current version 8 January 2025.

Digital Object Identifier 10.1109/OJCOMS.2024.3521008

Signal Detection in Intelligent Reflecting Surface-Assisted NOMA Network Using LSTM Model: A ML Approach

HALEEMA SADIA [1], HAFSA IQBAL [2] (Member, IEEE), SYED FAWAD HUSSAIN [3] (Senior Member, IEEE), AND NASIR SAEED [4] (Senior Member, IEEE)

[1]Department of Electrical and Communication Engineering, College of Engineering, United Arab Emirates University, Al Ain, UAE
[2]Autonomous Mobility and Perception Laboratory, University Carlos III of Madrid, 28911 Madrid, Spain
[3]School of Computer Science, University of Birmingham, Dubai, UAE
[4]Department of Electrical and Communication Engineering, United Arab Emirates University, Al Ain, UAE

CORRESPONDING AUTHORS: N. SAEED (e-mail: mr.nasir.saeed@ieee.org)

This work was supported by the Research Start Up Grant at United Arab Emirates University (UAEU) under Grant 12N129.

ABSTRACT Non-orthogonal multiple access (NOMA) is already considered a viable multiple access scheme in fifth-generation networks. However, the stochastic behaviour of a wireless channel becomes a key performance limiting factor. To combat this, and with the advancement of metasurface technology, NOMA networks are being integrated with intelligent reflecting surfaces (IRSs) to improve signal strength. But IRS complicates the detection accuracy of a NOMA system, which is dependent on the correctness of the successive interference cancelation (SIC) process. In this article, we propose a machine learning (ML)-based approach to perform joint channel estimation and signal detection in an IRS-enabled uplink NOMA network under efficient mitigation of SIC error propagation. The proposed scheme exploits a four layer deep learning (DL) model by employing a long short-term memory (LSTM) core structure. Further, to optimize the phase shifts of IRS, we exploit a low complexity iterative solution using the element-wise block coordinate descent (EBCD) method. Monte Carlo simulations are performed to analyze the performance of the proposed scheme, and the findings show a considerable improvement in channel estimation and signal detection using the LSTM based IRS-NOMA receiver. The comparison is made with a maximum likelihood detector employing conventional SIC scheme using least squares and minimum mean square error channel estimation approaches in a realistic path loss channel model with severe inter-symbol interference.

INDEX TERMS Non-orthogonal multiple access (NOMA), intelligent reflecting surface (IRS), machine learning (ML), signal detection, channel estimation, deep learning (DL), long short-term memory (LSTM).

I. INTRODUCTION

WITH the progressive development of fifth generation (5G) and beyond, the anticipated demands for enhanced spectral efficiency (SE), massive connectivity, higher reliability, and low communication latency have increased drastically [1]. In order to address the massive need of next-generation applications, new technologies are being investigated to provide fast and reliable data communication. The non-orthogonal multiple access (NOMA) scheme has already proven to be an effective multiple access scheme for the 5G and beyond 5G (B5G) wireless networks [2], [3], [4], providing improved performance in terms of connectivity, coverage, SE, energy efficiency (EE), and resource allocation [5], [6], [7].

By facilitating multiple users on a single resource, NOMA defies the concept of orthogonal multiple access techniques and offers a wide range of degrees of freedom (DoF) [8]. Additionally, it demonstrates great flexibility in terms of integrating with the key enabling technologies for 5G and B5G, including multiple-input

multiple-output (MIMO), cooperative communication, heterogeneous networks (HetNets), cognitive radio networks (CRNs), millimetre wave (mmWave) communication, and intelligent reflecting surfaces (IRSs) technology [9], [10], [11], [12]. However, in a multi-user environment, the stochastic behaviour of a wireless channel becomes one of the primary limiting factors for performance enhancement. To combat the random fluctuations of these wireless radio links, and with the progress in metasurfaces, IRSs appears as a passive albeit promising solution [13], [14], [15].

NOMA is generally classified into two distinct categories, namely, code domain NOMA (CD-NOMA) [16] and power domain NOMA (PD-NOMA) [17]. CD-NOMA multiplexes in the code domain by employing user-specific spreading sequences that are either sparse or non-orthogonal cross-correlation sequences with a low correlation coefficient [18]. Whereas, multiple users are served simultaneously, with varying power levels, in the PD-NOMA scheme [19], [20]. Hence, it offers a multi-user access system that provides an additional level of signal separation and base station (BS) access [21]. With the evolution towards heterogeneous and software controlled networks [22], the integration of IRS-enabled NOMA networks have the capability to improve performance gains in a dense user environment with diverse applications [23], [24], [25], [26]. The potential vision of reconfigurable environments unveils a new avenue for the researchers to investigate the integration of IRS with NOMA networks [12], [27].

An IRS is comprised of several low-cost passive metasurfaces that can be individually tweaked to control the phase and amplitude of incident signals [28]. The symmetric array of IRS elements provide flexible control of reflections using a low-cost IRS controller. By superimposing constructive/destructive signals at the receiving end through IRS, the received signal strength can be increased [29]. IRS differs from conventional relay technologies such as amplify-and-forward (AF), decode-and-forward (DF), and back-scatter communication [30], [31] and does not require any signal processing capabilities [32]. Therefore, combining these two complimentary technologies considerably improves the performance of NOMA communication systems. NOMA users attainable rates, sum rate, and EE can be maximized by using optimal passive IRS phase shift components [27], [33].

In conventional power domain (PD) NOMA systems, superposition coding (SC) is performed at the transmitter side based on varied power allocation, and successful interference cancelation (SIC) is performed at the receiving side [17]. The SC process introduces additional signal interference, which is removed on the receiving side by SIC. In NOMA systems the acquisition of channel state information (CSI) is critical for SIC performance, which becomes exceedingly difficult with IRS-enabled networks [34]. In case of imperfect SIC, the residual interference significantly degrades the performance of NOMA systems. Further, the detection accuracy of a network is highly dependent on the correctness of the SIC process, where multiple users are decoded in a sequential manner. The SIC process also suffers with the effects of error propagation in a real-time wireless channel which degrades the performance. With IRS enabled NOMA networks, the situation becomes more challenging due to multiple signal reflections and increased attenuation losses [35].

Therefore, to address the aforementioned challenges, ML particularly deep learning (DL) has gained considerable attention in wireless communication networks [36]. The anticipated demands of users escalates the system complexity for B5G networks; which brings the deep neural networks (DNNs) in frame and therefore are often a partial substitute in several communication configurations [37]. Previously, several studies have been done for channel estimation and signal detection in conventional NOMA networks through DL. Narengerile and Thompson in [38] investigated a DL-based uplink NOMA receiver for joint channel estimation and signal detection. The proposed receiver provide improved performance over the conventional maximum-likelihood detector (MLD). Emir et al. in [39] proposed a DL-based detector for joint channel estimation and signal detection under both perfect and imperfect CSI for multi-user orthogonal frequency division multiplexing (OFDM)-NOMA over Rayleigh fading channels. The proposed detector outperformed the conventional detectors both in offline and online training.

To reduce SIC error propagation and perform signal detection, Zhu et al. in [40] proposed a DL-based soft information receiver (DLSI) for uplink multiple-input-single-output (MISO)-NOMA networks. Emir et al. in [41] proposed a novel deep learning-aided multi-user detection (DeepMuD), to enable the machine type communication with enhanced error performance in uplink NOMA networks. To reduce system complexity, Chitti et al. in [42] investigated a MuD based on DNN. The MuD approach outperformed conventional detectors with the least complexity. Gui et al. in [43] also proposed a novel DL enabled NOMA system to serve multiple random deployed users with single BS. To provide end-to-end simultaneous transmissions with channel estimation, equalization, and demodulation, Xie et al. in [44] developed a novel receiver based on DL for NOMA signal detection. However, when NOMA networks are aided with IRS, the channel estimation and signal detection become more complicated because of dual channel paths. Hence, it has become very challenging to estimate the channels of large-dimensional intelligent surfaces having multiple passive reflecting elements. This constraint puts a major limit on the effective deployment of IRSs in NOMA networks due to computational cost and complexity.

For realizable systems, few studies have recently proposed DL-based estimation and detection models for IRS-assisted frameworks, which reduce the complexity and mitigate error propagation issues [35], [45], [46]. Taha et al. in [47] addressed training overhead and hardware complexity of large intelligent surfaces through a DL-based solution. Jiang et al. in [48] performed channel estimation by collecting real data from IRS active elements to train the

DNNs. Inspired by this, the authors in [49] proposed an intelligent receiver model for IRS-assisted cognitive-NOMA network by employing a DL approach, thus resulting in improved channel estimation and signal detection. However, the investigation of channel estimation and signal detection in IRS-enabled uplink NOMA networks by employing ML-based signal detection techniques needs to be investigated.

Based on the potential advantages of IRS and the exploitation of DL in a reconfigurable environment, we have proposed a low complexity ML approach for channel estimation and signal detection in an uplink IRS-assisted orthogonal frequency division multiplexing (OFDM)-NOMA network. Using the proposed model, channel estimation and signal detection is performed more effectively in a complex fading environment with least SIC error propagation. The following are the article's key contributions:

- We propose a low complexity ML-based approach for an uplink IRS-assisted OFDM-NOMA framework to perform joint channel estimation and signal detection. The proposed scheme exploits a four layer DL model based on a long short-term memory (LSTM) core structure. Moreover, a less complex iterative approach, i.e., the element-wise block coordinate descent (EBCD) method, is embedded in the framework to optimize the IRS phase shifts.
- We investigate the ML-based MuD receiver in a NOMA network employing a distance-dependent fading path-loss channel model with severe intersymbol interference under optimized IRS phase shifts and also compare its performance to a conventional NOMA system without IRS scenario. The proposed model demonstrate a high accuracy with least loss error.
- We evaluate the performance of the proposed framework with minimum signal-to-interference-plus-noise ratio (SINR) requirements in terms of symbol error rate (SER) formulations. The simulation results are benchmarked with maximum-likelihood detector (MLD) under perfect CSI and conventional SIC scheme by employing least squares (LS) and minimum mean square error (MMSE) channel estimation approaches under imperfect CSI scenario.

A. MANUSCRIPT ORGANIZATION AND NOTATIONS

The remaining of the manuscript is organized as follows: Section II describes the IRS-enabled network model alongwith problem formulation. Section III discuses the LSTM model for MuD in uplink IRS-assisted NOMA transmission. The simulation results and analysis are presented in Section IV, and Section V concludes the work.

Notations: The italic light letters (h), boldface lowercase letters ($\mathbf{h}$), and uppercase boldface letters ($\mathbf{H}$) in this work represent scalars, vectors, and matrices, respectively. The absolute square and Hermitian are represented by the symbols $|\cdot|^2$ and $(\cdot)^H$, respectively. Complex Gaussian random variables are denoted as $\mathcal{CN}$ while complex spaces characterized by n dimensions are represented by the notation $\mathbb{C}^{(\cdot)}$. The symbols diag$(\cdot)$, $\sum(\cdot)$, $\mathbb{E}[\cdot]$, and $\mathbb{R}[\cdot]$ represents the diagonal matrix, summation operator, statistical expectation of random variables, and real part of a complex value, respectively.

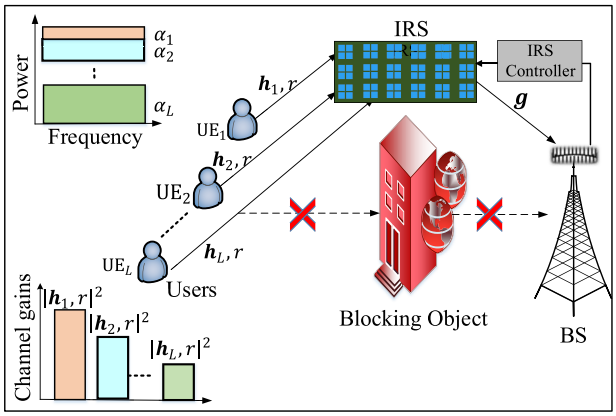

FIGURE 1. System model of uplink IRS-assisted NOMA network.

II. IRS-ENABLED NOMA NETWORK MODEL

For IRS-assisted uplink single-input-single-output (SISO)-NOMA transmission, we investigate the system model presented in Fig. 1. An IRS made up of R reflecting components is placed between the BS and the user equipments (UEs) to facilitate the users lying in dead zone, i.e., no direct signal path exists between the users and BS. The location of BS and IRS is assumed to be fixed, but the UEs position may be dynamic. The IRS is equipped with a low-power controller to perform coordination between BS and IRS through a backhaul link. For simultaneous data transmission, an OFDM modulation scheme having N-subcarriers with L users per subcarrier is presumed. Assuming that $s_j(n)$ is the baseband symbol of j_{th} user with normalized power as $\mathbb{E}\{|s_j(n)|^2\} = 1$, then the intended signal at each user end is represented as

$$x(n) = \sqrt{P_t \alpha_j(n)} s_j(n), \tag{1}$$

where P_t is the total power allocated to each of the N-subcarriers and α_j is the NOMA power allocation coefficient for j_{th} users such that $\alpha_j(n) = P_j(n)/P_t$, subject to $\sum_{j=1}^{L} \alpha_j(n) = 1$ for $\forall j \in L$ with $P_j(n)$ as the transmission power allocated to j_{th} user on n_{th} subcarrier. The signal received at the BS after reflection from IRS on n_{th} subcarrier is given by

$$\begin{aligned} y_k(n) &= f_{k,r}(n)x(n) + z_k(n), \quad k \in \{1, 2, \ldots, L\}, \\ &= f_{k,r}(n) \sum_{j=1}^{L} \sqrt{P_t \alpha_j(n)} s_j(n) + z_k(n). \end{aligned} \tag{2}$$

The factor $f_{k,r}(n)$ represents the two-fold channel gain, which is expressed as

$$f_{k,r}(n) = \mathbf{g}(n)\Theta(n)\mathbf{h}_{j,r}(n), \quad k \in \{1, 2, \ldots, L\}, \tag{3}$$

where $\mathbf{g} \in \mathbb{C}^{1\times R}$ indicates the channel gains between BS and IRS, and $\mathbf{h}_{j,r} \in \mathbb{C}^{R\times 1}$ shows the channel gains between IRS and UE's. The reflection matrix for IRS is defined as $\Theta \in \mathbb{C}^{R\times R}$ and comprises the information of the amplitude as well as the phase shift coefficients of IRS, which is represented as follows:

$$\Theta(n) = \text{diag}\Big(\gamma_1 e^{j\vartheta_1}, \gamma_2 e^{j\vartheta_2}, \ldots, \gamma_R{}^{j\vartheta_R}\Big). \tag{4}$$

Here, $\gamma_1, \gamma_2, \ldots, \gamma_R \in [0, 1]$ denote the amplitude reflection coefficient. In the literature, this coefficient is frequently considered fixed to reduce the hardware complexity overhead [28]. The phase reflection coefficients are given by $\vartheta_1, \vartheta_2, \ldots, \vartheta_R \in [0, 2\pi)$. The factor $z_k(n) \sim \mathcal{CN}(0, \sigma_k^2(n))$ represents the complex symmetric Gaussian noise with zero mean and variance σ_k^2. For simplicity, albeit without loss of generality we consider a single cell with two users; thus, received signals at near user (UE_1) and far user (UE_2) are given respectively by $y_k(n),\ k = \{1, 2\}$.

III. PROPOSED METHODOLOGY

For detection of intended users' symbols from the received signal, we study a DL-based receiver in this section. Furthermore, to obtain phase shifts of IRS, a low complexity iterative suboptimal solution based on the EBCD optimization algorithm is employed. The NOMA power allocation assignment is assumed on ascending users' channel ordering, where CSI is obtained via channel estimation.

A. ELEMENT-WISE BLOCK COORDINATE DESCENT APPROACH FOR IRS PHASE SHIFTS

Firstly, the IRS phase shifts are obtained with an iterative approach, i.e., EBCD method. For brevity, we optimize phase shifts by considering the rate of near user only. Hence, for a single cell with two users; the SNR expression for near user is given by

$$\Gamma_1 = \frac{\sqrt{P_t\alpha_1}|f_{1,r}(n)|^2}{\sigma^2(n)}. \tag{5}$$

From (5), the desired maximization problem is defined as

$$\max_{\vartheta} \ |f_{1,r}(n)|^2 \tag{6a}$$
$$\text{s.t.} \ \ |\vartheta_i| = 1, \quad i \in \{1, 2, \ldots, R\}. \tag{6b}$$

To solve (6), we first convert it into a tractable form. Let

$$\mathbf{v} = [v_1, \ldots, v_R]^H \text{ and } v_i = e^{j\vartheta_i}, \ \forall i \in R.$$

Furthermore, consider that

$$\mathbf{v}^H\mathbf{a}_k(n) = \mathbf{g}(n)\Theta(n)\mathbf{h}_{k,\text{r}}(n).$$

where

$$\mathbf{a}_k(n) = \text{diag}\big(\mathbf{h}_{k,\text{r}}(n)\big)^H\mathbf{g}(n) \in \mathbb{C}^{R\times 1}.$$

The fully separable phase shifts of all elements make it possible to solve (6) via an iterative solution. To this end, we adopt the suboptimal EBCD method to optimize the phase shifts by iteratively optimizing each element of $\mathbf{v}$, i.e., $v_i,\ \forall i \in R$ given the other phase shifts as, $v_l,\ \forall l \in R$, where $l \neq i$ in the absence of direct channel links. With fixed v_l, we formulate (6) as follows;

Algorithm 1 EBCD Method for IRS Phase Optimization

Input: iteration number r, feasible solution v_i, stopping criteria $\varepsilon > 0$;
Output: Optimal solution v_i^*;
Set $r = 0$ and initialize $v_i = v_i^{(0)}$;
repeat
  for $i = 1{:}R$
    Calculate v_i^* using (13), $\forall i \in R$;
  end
Update v_i^* and keep v_l unchanged, i.e., $v_l^r = v_l^{r-1}, \forall l \neq i$;

Perform iterations $r = r + 1$ until stopping criteria met.

$$\max_{\mathbf{v}} \ v\mathbf{U}v^H + 2\mathbb{R}\{v\theta\} + A \tag{7a}$$
$$\text{s.t.} \ \ |v_i| = 1, \quad i \in \{1, 2, \ldots, R\}, \tag{7b}$$

where

$$\mathbf{U} = \sum_k \mathbf{a}_k\mathbf{a}_k^H, \ \forall k, \tag{8}$$

$$\theta_i = \sum_{l\neq m}^{R} \mathbf{U}(l, m)v_i^H - \tilde{\boldsymbol{\theta}}(l), \tag{9}$$

$$A = \mathbf{U}(l, l) - 2\mathbb{R}\sum_{l\neq m}^{R} v_m\tilde{\boldsymbol{\theta}}(m), \tag{10}$$

$$\tilde{\boldsymbol{\theta}} = \sum_k \mathbf{a}_k, \ \forall k. \tag{11}$$

Using algebraic properties, (7) becomes a simplified update rule as follows;

$$\max_{v_i} \ 2\mathbb{R}\{v_i\theta_i\} \tag{12a}$$
$$\text{s.t.} \ \ |v_i| = 1, \quad i \in \{1, 2, \ldots, R\}. \tag{12b}$$

Hence, by fixing $v_l,\ \forall l \in R, l \neq i$, the optimal solution to the above problem becomes

$$v_i^* = \frac{\theta_i^H}{|\theta_i|}, \ \forall i. \tag{13}$$

By iteratively optimizing each block of $R - 1$ phase shifts and fixing the other R phases, the optimal phase shifts can be obtained based on the update rule of (13). Algorithm 1 provides the pseudo-code for the EBCD approach for IRS phase shift optimization.

B. ML MODEL FOR IRS-NOMA RECEIVER

For the proposed framework of Section II, here a DL-based model with long short-term memory (LSTM) layers and fully linked layers is employed for channel estimation and user symbol detection at the BS in a one-shot process. The

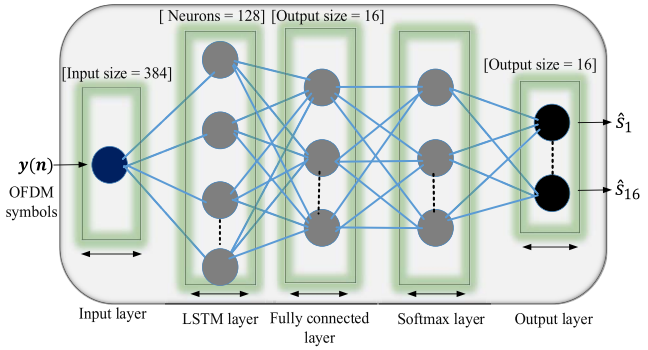

FIGURE 2. DL model of uplink IRS-OFDM-NOMA receiver.

proposed model can effectively capture temporal dependencies and long-range correlations in OFDM-NOMA packets, which are critical for accurate channel estimation and signal detection. To train ML model, data is provided in the form of OFDM-NOMA packets with a total of 64 subcarriers, with one packet transmitted per subcarrier. Each OFDM packet has 2 pilot symbols for channel estimation and 1 data symbol containing the SC signals of near and far users. Quadrature phase shift keying (QPSK) with 2 bits per subcarrier is used for baseband modulation, while the OFDMA technique is employed for passband modulation. The inverse discrete Fourier transform (IDFT) is used to create OFDM orthogonal carriers. A cyclic prefix (CP) with a predetermined length is inserted as a guard interval to counteract inter-symbol interference (ISI). After performing OFDM modulation, packets are transmitted to BS through an IRS reflected wireless radio link. The phase shifts of IRS are tuned via low computational micro-controller. With AWGN noise, the BS gets both users' two-path reflected overlaid signals.

The ML model is trained for a given feature vector $\mathbf{y}(n)$ that contains both the real and imaginary components of the OFDM symbol, by using the OFDM packets received from NOMA users. With 64 subcarriers and 3 OFDM symbols per subcarrier, the total number of input features used is 384. Labels are assigned to transmitted symbols by considering QPSK modulation. The architecture of DL model as illustrated in Fig. 2, comprises of 4 main layers having an LSTM core layer with an input size of 384 and output size of 128. The LSTM layer take advantage of the OFDM data's temporal dependency, and the OFDM subcarriers are considered time steps that assist the ML-model in obtaining relevant data from channel acquisition. The next layer is a fully connected layer with an output size of 16, which works independently on each time step in the LSTM-based DL model. Following that, a softmax layer is introduced to extract data from a fully connected layer. The softmax activation function transforms the fully connected layer output into a normalized vector of $[0, 1]$. The classification layer is used in the final stage to get output vector, followed by terminal layers with output sizes

Algorithm 2 LSTM Model

Preprocessing:
Total Samples = 560000; cross-validation = 6: 4;
Training data: X;
Training data labels: X_l;
Framework of DL Model:
Input layer: LSTM {input: 384; output: 128};
Hidden layer: 128 neurons;
Output layers: output size 16;
Training of DL Model:
for $i = 1$: No. of epochs
$x_k = \text{randperm}(n)$
for $j = 1$: No. of mini − batches
$\text{batch}_X = X[x_k[(j-1) \times \text{m} + 1 : j \times \text{m}], :]$;
$\text{batch}_{X_l} = X_l[x_k[(j-1) \times \text{m} + 1 : j \times \text{m}], :]$;
end
end
Testing of DL Model: Evaluate trained DL model for real testing data;
Output: user's symbols;

equal to the number of classes, i.e., 16. The loss function for detecting each user symbol in the given network is given by;

$$f_{\text{loss}} = \frac{1}{\mathcal{L}} \sum_{\tau=1}^{\mathcal{L}} |(s_k(\tau) - \hat{s}_k(\tau)|^2, \tag{14}$$

here $\mathcal{L}$ denotes the number of training OFDM packets, $s_k(\tau)$ denotes the target output, and $\hat{s}_k(\tau)$ shows the predicted output at the response τ, respectively. The model is trained offline using simulated data and then tested online to confirm MuD's performance under certain channel conditions. The pseudo-code for the investigated LSTM model is provided in Algorithm 2.

IV. SIMULATION RESULTS AND DISCUSSION

This section provides the simulation results to demonstrate the channel estimation and symbol detection through ML-based scheme. The DL model is trained offline using simulation data and evaluated with the dynamic data in an online phase. For performance analysis, the proposed receiver is compared to conventional SIC and MLD algorithms. Because the static deployment of IRS provides a line-of-sight (LoS) connection between BS and IRS, the Rician channel model is employed for two-fold channel pathways given as

$$\mathbf{g}(n) = \sqrt{\left(\frac{d}{d_0}\right)^{-\eta_1}} \left(\sqrt{\frac{\kappa}{1+\kappa}} \tilde{\mathbf{g}}(n)^{\text{LoS}} + \sqrt{\frac{1}{1+\kappa}} \tilde{\mathbf{g}}(n)^{\text{NLoS}} \right). \tag{15}$$

Similarly, the channel paths between IRS and users are expressed by non-line of sight (NLoS) Rayleigh channel

TABLE 1. Simulation parameters.

Parameter	Value	Parameter	Value
L (no. of users)	2	R (IRS elements)	32, 64
d_1 (UE_1 to IRS)	6 m	d_2 (UE_2 to IRS)	10 m
d (IRS to BS)	5 m	N(OFDM subcarriers)	64
Length of CP	24, 32	DL model layers	4
Training samples	400000	Testing samples	160000
Optimizer	Adam	Learning rate	0.1
Mini-batch size (m)	4000	No. of epochs	50
Modulation scheme	Baseband: (QPSK), Passband: (OFDM)	Path loss(η_1, η_2)	2 (BS to IRS), 3 (IRS to Users)

model

$$\mathbf{h}_{k,\mathrm{r}}^{H}(n) = \sqrt{\left(\frac{d_{1,2}}{d_0}\right)^{-\eta_2}}\left(\sqrt{\frac{\kappa}{1+\kappa}}\left(\tilde{\mathbf{h}}_{k,\mathrm{r}}^{H}\right)^{\mathrm{LoS}} + \sqrt{\frac{1}{1+\kappa}}\left(\tilde{\mathbf{h}}_{k,\mathrm{r}}^{H}\right)^{\mathrm{NLoS}}\right), \tag{16}$$

where $d_0 = 1\mathrm{m}$ is the reference distance, d and $d_{1,2}$ represents the respective distances from BS to IRS and IRS to UEs, and $\eta_{\{1,2\}}$ shows the path loss exponents of the individual links, respectively. Further, we consider the Rician factor $\kappa = 5$ dB. $\tilde{\mathbf{g}}^{\mathrm{LoS}}$, $(\tilde{\mathbf{h}}_{k,\mathrm{r}}^{H})^{\mathrm{LoS}}$ and $\tilde{\mathbf{g}}^{\mathrm{NLoS}}$, $(\tilde{\mathbf{h}}_{k,\mathrm{r}}^{H})^{\mathrm{NLoS}}$ represent the LoS and non-LoS components of channel links, respectively. To estimate the wireless channel links under imperfect CSI (ipCSI), conventional LS [50] and MMSE [51] schemes are employed. The parameters used in the simulations are listed in Table 1. The MATLAB computing environment is used to develop the DL model. We created 400, 000 samples for training and 160, 000 samples for testing, taking into consideration the performance efficiency of LSTM model. The training is executed on a Core i7-7500U CPU.

First, we analyze the accuracy and loss error of the proposed DL model in Fig. 3 and Fig. 4, respectively. Fig. 3 shows the prediction accuracy of the correct outcomes. The training accuracy (solid line) rises fast in the beginning and reaches the highest point. The validation accuracy (dashed line) follows the training accuracy closely, which further demonstrates that the model is not over-fitting the training data. The stable level of both training and validation accuracy, which stay around 97%, after about 400 iterations. This high accuracy, which lasts for the 50 epochs, proves that the model performs well and keeps its performance. Furthermore, the substantial fluctuations observed around 3000 iterations demonstrate the attainment of the global minima by the proposed approach. Fig. 4 shows the loss error of the proposed model during the training and validation process. As demonstrated by the curves, the training loss (solid line) and validation loss (dashed line) both drop quickly within the first few hundred iterations, showing

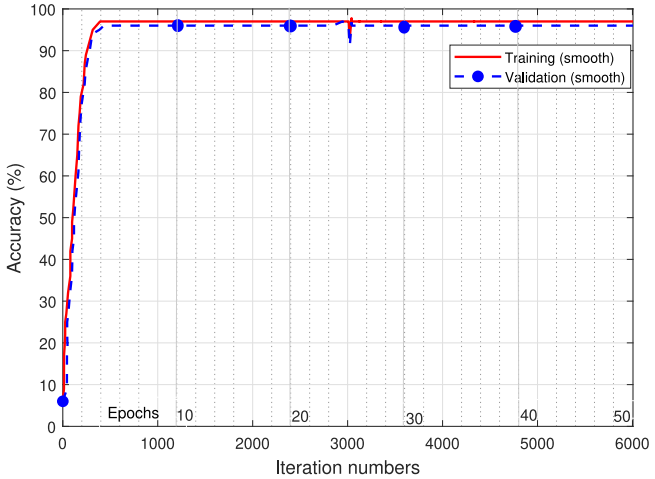

FIGURE 3. Accuracy curve of proposed DL model.

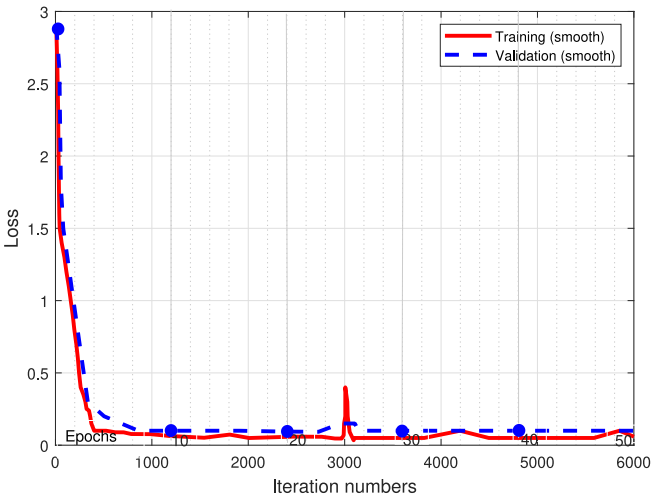

FIGURE 4. Loss error curve of proposed DL model.

that the model is learning fast from the training data and the error is decreasing. After around 400 iterations, the loss becomes low and steady at a minimum value of 0.1 for the rest of the training process. This low value and stable loss, along with high accuracy, show that the proposed LSTM model not only reduces errors quickly but also maintains high efficiency during the training process.

Fig. 5 shows the SER performance curves of single cluster users, i.e., near (UE_1) and far (UE_2) users, using the LSTM-based receiver versus conventional MLD receiver under the IRS-aided network. The comparison is also performed in the absence of the IRS scenario, in which the system model is reduced to a conventional wireless network. As a result, in the presence of obstacles and practical path loss channel model concerns, users employ direct communication links. When users are assisted with IRS, the simulation curves show a substantial improvement of 5dB under ipCSI in performance. This demonstrate that IRS-enabled networks succeed to improve the performance of both users under path

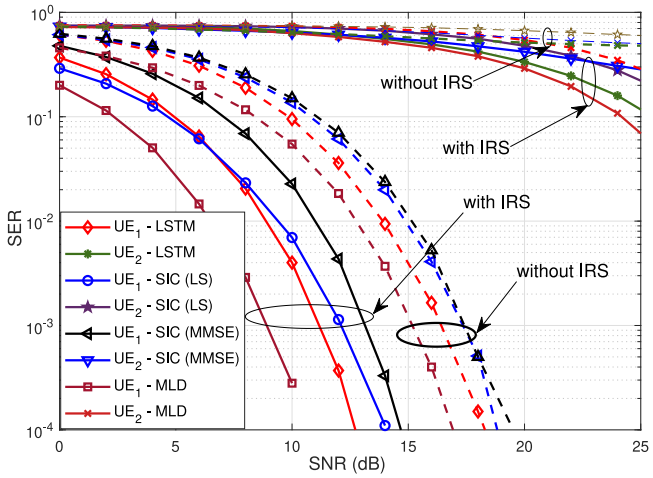

FIGURE 5. SER versus SNR (dB) with LSTM-based and conventional receiver comparison for UE_1 and UE_2 with IRS and without IRS-aided NOMA network.

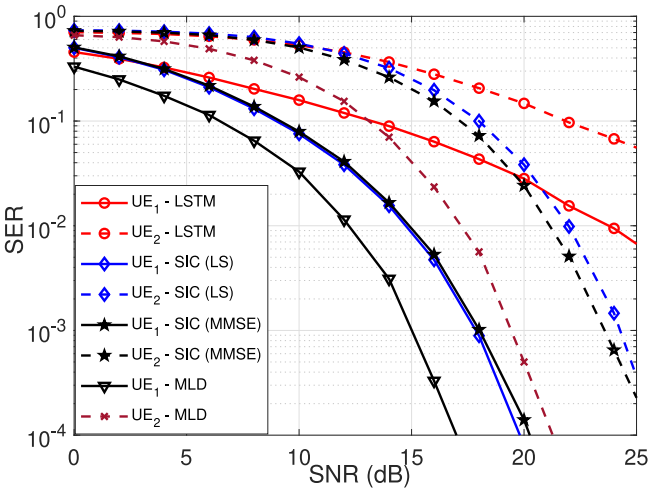

(a) SER versus SNR (dB) with IRS=32

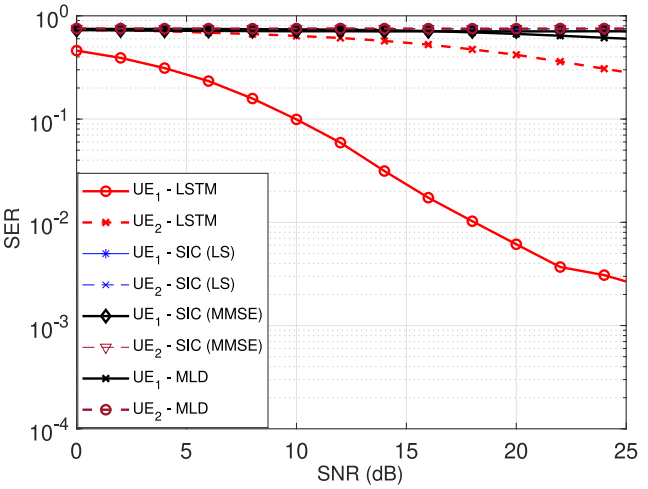

(b) SER versus SNR (dB) with IRS=64

FIGURE 6. SER versus SNR (dB) comparison for UE_1 and UE_2 with different IRS elements.

loss channel models. The second key finding is the improved user performance with the DL-based receiver, particularly for a far-distance user with poor channel conditions. The inter symbol interference reduces with a fixed CP length of 32, and the MLD under perfect CSI (pCSI) achieves the best possible performance curves with the lowest SER, as shown in Fig. 5. The far user's performance degrades substantially when using traditional SIC scheme via LS and MMSE approaches, but with the LSTM based receiver, the far user achieves better results. The fact behind is that the SIC error propagation in case of DL-based approach reduces to a minimum, resulting in improved SER performance curves. To further investigate the performance analysis of the proposed LSTM-based model, various aspects are presented below.

A. IMPACT OF IRS ELEMENTS

The effect of IRS elements on the SER performance curves with ML-based receiver is examined in this section. Two alternative symmetric arrays of IRS elements, 32 and 64, are used to emulate the considered uplink model. Fig. 6(a), and Fig. 6(b) show the efficiency of the LSTM-based receiver for near and far users under different number of IRS elements, respectively. Conventionally, increasing the number of IRS elements R, introduces more reflected signals, which improves information reflections at the intended receiver end. Furthermore, it confirms the performance gain obtained by introducing a constant number of IRS elements in a conventional NOMA framework without IRS scenario. Additionally, it underscores the effectiveness of enhancing spatial multiplexing of the network by increasing the number of low-cost IRS elements, compared to the number of high-cost transmit and receive antennas [3], [4]. However, with an increased number of IRS elements, the channel estimation becomes very challenging which results in the poor performance of a conventional SIC receivers as shown in Fig. 6. Here, the LSTM model provides enhanced performance curves for both users as compared to conventional SIC approach via LS and MMSE, by performing channel estimation efficiently as depicted in Fig. 6(b).

B. IMPACT OF CP LENGTH

In conventional OFDM systems the orthogonality of sub-carriers is maintained by inserting a CP of fixed length. The presence of intersymbol interference (ISI) in OFDM signals will cause an error in receiving bits of information on the receiver side. With IRS-enabled NOMA networks, the effect of multipath propagation increases, as the transmitter signal travels via dual reflected paths to the receiver. Thus, it enhances symbol error propagation during the SIC process, thereby interfering with the correct detection of symbols. Here, the use of CP is critical to the reliability of the OFDM signals. To prevent OFDM signals from ISI, the CP functions as a buffer region or guard interval. By varying the length

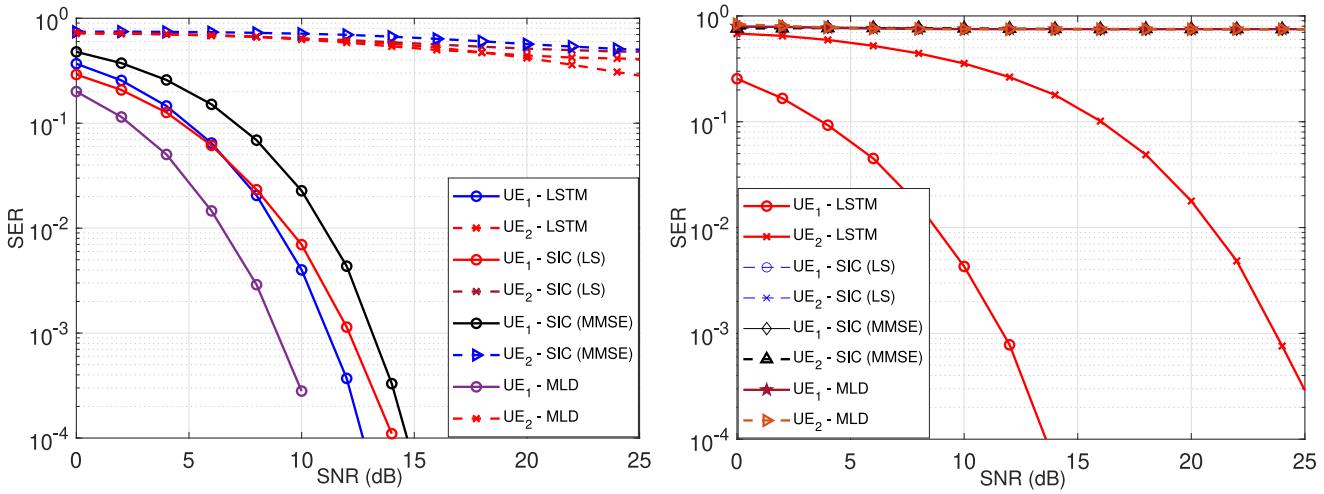

(a) SER versus SNR (dB) with CP=32

(b) SER versus SNR (dB) with CP=24

FIGURE 7. Comparison of SER versus SNR (dB) for UE_1 and UE_2 with different CP lengths.

of CP, the performance curves show variations, as shown in Fig. 7(a) and Fig. 7(b). Here, we consider two different CP length, i.e., 32 and 24. The results demonstrate that when the length of CP is equal to channel response, the performance of near user increases significantly but this is done at the cost of far user performance degradation, as shown in Fig. 7(a). Similarly, when the CP length becomes very short, the ISI becomes very dominant; therefore, the performance of conventional SIC scheme degrades drastically resulting in poor performance of MLD. Here, the LSTM-based receiver works efficiently and provides better results under severe ISI as shown by performance curves in Fig. 7(b).

C. IMPACT OF CHANNEL BEHAVIOUR

In a practical wireless communication environment, the signal suffers with multipath fading effects which degrades the performance. With IRS-enabled NOMA networks the dual paths introduces more multipath reflections, hence interference becomes more prominent and SIC performance degrades. To further scrutinise the robustness of the LSTM-based receiver, we investigate the formulated framework under LoS as well as NLoS fading channel models. The comparison is made by considering the Rician (Ric) (LoS) and Rayleigh (Ray) (NLoS) wireless channel models using Monte Carlo simulations, as shown in Fig. 8. The performance of the Rician channel model is significantly better than that of the Rayleigh channel due to the presence of a line of sight component. Moreover, the LSTM model provides better results under the Rayleigh fading model at low SNR, but the performance degrades at higher SNR values, as compared to conventional receiver using SIC via LS and MMSE channel estimation schemes. It shows that the DL model performs better under LoS channel conditions, which is a substantial assumption in IRS-empowered wireless transmission networks due to IRS static deployment.

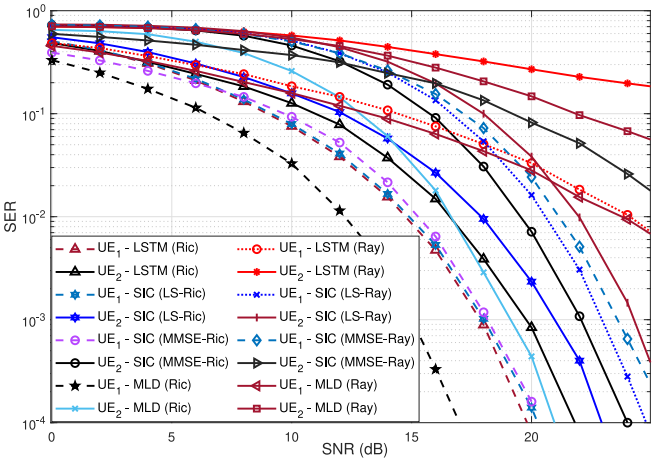

FIGURE 8. Comparison of SER versus SNR (dB) with LSTM-based receiver for UE_1 and UE_2 under LoS and NLoS fading channel models.

V. CONCLUSION AND FUTURE DIRECTIONS

In this paper, a DL-based model is leveraged for an uplink IRS-assisted OFDM-NOMA network. LSTM based receiver employs the sequential OFDM symbols in a single shot process to perform joint channel estimation and signal detection. The DL model is trained offline with the optimal IRS phase shifts obtained through EBCD by keeping the trade-off in performance and complexity. The results indicate that the improved performance is attained with low complexity LSTM-based receiver in IRS-enabled NOMA network, where channel estimation becomes more challenging. When ISI is greater, the LSTM-based receiver provides better signal detection as compared to the conventional SIC scheme. Moreover, performance analysis of the proposed receiver is provided under LoS and NLoS channel conditions for uplink wireless communication networks.

The investigated work highlights the potential of integrating IRS with NOMA to enhance connectivity by

improving signal strength and coverage for 6G networks. The proposed LSTM-based approach can effectively facilitates Ultra-Reliable Low-Latency Communications (URLLC) and Massive Machine-Type Communications (mMTC), proving advantageous for applications such as autonomous vehicles, smart cities, and extensive IoT networks. However, the proposed approach also presents challenges related to computational complexity and scalability in large networks, as well as issues concerning robustness in dynamic environments and integration with current 5G infrastructure. Future research should focus on the development of more efficient DL algorithms and the assurance of compatibility for seamless deployment. The proposed approach can be extended for the investigation of massive multi-antenna environment with multiple IRSs deployment. The presented frameworks can also be investigated further using different DL-based NOMA power allocation and IRS phase optimization algorithms for multi-user interference scenarios.

REFERENCES

[1] M. M. d. Silva and J. Guerreiro, "On the 5G and beyond," *Appl. Sci.*, vol. 10, no. 20, p. 7091, Oct. 2020.

[2] Y. Liu, Z. Qin, M. Elkashlan, Z. Ding, A. Nallanathan, and L. Hanzo, "Nonorthogonal multiple access for 5G and beyond," *Proc. IEEE*, vol. 105, no. 12, pp. 2347–2381, Dec. 2017.

[3] H. Sadia, A. K. Hassan, Z. H. Abbas, G. Abbas, M. Waqas, and Z. Han, "IRS-enabled NOMA communication systems: A network architecture primer with future trends and challenges," *Digit. Commun. Netw.*, vol. 10, no. 5, pp. 1503–1528, 2024.

[4] H. Sadia, A. K. Hassan, Z. H. Abbas, G. Abbas, and J. M. Cioffi, "An IRS-enabled phase cooperative framework for sum rate maximization in B5G networks," *IEEE Trans. Netw. Sci. Eng.*, early access, Nov. 6, 2024, doi: 10.1109/TNSE.2024.3486733.

[5] J. Niu, S. Zhang, K. Chi, G. Shen, and W. Gao, "Deep learning for online computation offloading and resource allocation in NOMA," *Comput. Netw.*, vol. 216, Oct. 2022, Art. no. 109238.

[6] Z. Chen, Z. Ding, X. Dai, and R. Zhang, "An optimization perspective of the superiority of NOMA compared to conventional OMA," *IEEE Trans. Signal Process.*, vol. 65, no. 19, pp. 5191–5202, Oct. 2017.

[7] U. S. S. S. Arachchillage, D. N. K. Jayakody, S. K. Biswash, and R. Dinis, "Recent advances and future research challenges in non-orthogonal multiple access for 5G networks," in *Proc. IEEE 87th Veh. Technol. Conf. (VTC)*, 2018, pp. 1–6.

[8] H. Viswanathan and M. Weldon, "The past, present, and future of mobile communications," *Bell Labs Tech. J.*, vol. 19, pp. 8–21, Aug. 2014, doi: 10.15325/BLTJ.2014.2335491.

[9] Z. Ding, F. Adachi, and H. V. Poor, "The application of MIMO to non-orthogonal multiple access," *IEEE Trans. Wireless Commun.*, vol. 15, no. 1, pp. 537–552, Jan. 2016.

[10] L. Zhu, Z. Xiao, X.-G. Xia, and D. O. Wu, "Millimeter-wave communications with non-orthogonal multiple access for B5G/6G," *IEEE Access*, vol. 7, pp. 116123–116132, 2019.

[11] Z. Ding and H. V. Poor, "A simple design of IRS-NOMA transmission," *IEEE Commun. Lett.*, vol. 24, no. 5, pp. 1119–1123, May 2020.

[12] H. Sadia, A. K. Hassan, Z. H. Abbas, and G. Abbas, "System throughput maximization in IRS-assisted phase cooperative NOMA networks," *Phys. Commun.*, vol. 58, Jun. 2023, Art. no. 102007.

[13] C. Liaskos, S. Nie, A. Tsioliaridou, A. Pitsillides, S. Ioannidis, and I. Akyildiz, "Realizing wireless communication through software-defined HyperSurface environments," in *Proc. IEEE 19th Int. Symp. World Wireless, Mobile Multimedia Netw. (WoWMoM)*, 2018, pp. 14–15.

[14] W. Tang et al., "Wireless communications with reconfigurable intelligent surface: Path loss modeling and experimental measurement," *IEEE Trans. Wireless Commun.*, vol. 20, no. 1, pp. 421–439, Jan. 2021.

[15] H. Sadia, Z. H. Abbas, A. K. Hassan, and G. Abbas, "Outage probability analysis of reconfigurable intelligent surface (RIS)-enabled NOMA network," in *Proc. 10th Int. Conf. Wireless Netw. Mobile Commun. (WINCOM)*, 2023, pp. 1–6.

[16] M. Rebhi, K. Hassan, K. Raoof, and P. Chargé, "Sparse code multiple access: Potentials and challenges," *IEEE Open J. Commun. Soc.*, vol. 2, pp. 1205–1238, 2021.

[17] H. Sadia, M. Zeeshan, and S. A. Sheikh, "Performance analysis of downlink power domain NOMA under fading channels," in *Proc. IEEE ELEKTRO*, 2018, pp. 1–6.

[18] M. T. P. Le, L. Sanguinetti, E. Bjornson, and M.-G. Di Benedetto, "Code-domain NOMA in massive MIMO: When is it needed?" *IEEE Trans. Veh. Technol.*, vol. 70, no. 5, pp. 4709–4723, May 2021.

[19] M. Abd-Elnaby, G. G. Sedhom, E.-S. M. El-Rabaie, and M. Elwekeil, "NOMA for 5G and beyond: Literature review and novel trends," *Wireless Netw.*, vol. 26, pp. 1629–1653, May 2023.

[20] U. Ghafoor, M. Ali, H. Z. Khan, A. M. Siddiqui, and M. Naeem, "NOMA and future 5G & B5G wireless networks: A paradigm," *J. Netw. Comput. Appl.*, vol. 204, Aug. 2022, Art. no. 103413.

[21] Y. Liu, W. Yi, Z. Ding, X. Liu, O. A. Dobre, and N. Al-Dhahir, "Developing NOMA to next generation multiple access: Future vision and research opportunities," *IEEE Wireless Commun.*, vol. 29, no. 6, pp. 120–127, Dec. 2022.

[22] C.-H. Liu and D.-C. Liang, "Heterogeneous networks with power-domain NOMA: Coverage, throughput, and power allocation analysis," *IEEE Trans. Wireless Commun.*, vol. 17, no. 5, pp. 3524–3539, May 2018.

[23] L. Dong and H.-M. Wang, "Enhancing secure MIMO transmission via intelligent reflecting surface," *IEEE Trans. Wireless Commun.*, vol. 19, no. 11, pp. 7543–7556, Nov. 2020.

[24] C. Huang, A. Zappone, G. C. Alexandropoulos, M. Debbah, and C. Yuen, "Reconfigurable intelligent surfaces for energy efficiency in wireless communication," *IEEE Trans. Wireless Commun.*, vol. 18, no. 8, pp. 4157–4170, Aug. 2019.

[25] X. Yu, D. Xu, Y. Sun, D. W. K. Ng, and R. Schober, "Robust and secure wireless communications via intelligent reflecting surfaces," *IEEE J. Sel. Areas Commun.*, vol. 38, no. 11, pp. 2637–2652, Nov. 2020.

[26] Z. Zhang, C. Zhang, C. Jiang, F. Jia, J. Ge, and F. Gong, "Improving physical layer security for reconfigurable intelligent surface aided NOMA 6G networks," *IEEE Trans. Veh. Technol.*, vol. 70, no. 5, pp. 4451–4463, May 2021.

[27] X. Mu, Y. Liu, L. Guo, J. Lin, and N. Al-Dhahir, "Exploiting intelligent reflecting surfaces in NOMA networks: Joint beamforming optimization," *IEEE Trans. Wireless Commun.*, vol. 19, no. 10, pp. 6884–6898, Oct. 2020.

[28] Q. Wu, S. Zhang, B. Zheng, C. You, and R. Zhang, "Intelligent reflecting surface-aided wireless communications: A tutorial," *IEEE Trans. Commun.*, vol. 69, no. 5, pp. 3313–3351, May 2021.

[29] E. Basar, M. Di Renzo, J. De Rosny, M. Debbah, M.-S. Alouini, and R. Zhang, "Wireless communications through reconfigurable intelligent surfaces," *IEEE Access*, vol. 7, pp. 116753–116773, 2019.

[30] A. N. Parks, A. Liu, S. Gollakota, and J. R. Smith, "Turbocharging ambient backscatter communication," *ACM SIGCOMM Comput. Commun. Rev.*, vol. 44, no. 4, pp. 619–630, 2014.

[31] E. Björnson, Ö. Özdogan, and E. G. Larsson, "Intelligent reflecting surface versus decode-and-forward: How large surfaces are needed to beat relaying?" *IEEE Wireless Commun. Lett.*, vol. 9, no. 2, pp. 244–248, Feb. 2020.

[32] C. Huang et al., "Holographic MIMO surfaces for 6G wireless networks: Opportunities, challenges, and trends," *IEEE Wireless Commun.*, vol. 27, no. 5, pp. 118–125, Oct. 2020.

[33] F. Fang, Y. Xu, Q.-V. Pham, and Z. Ding, "Energy-efficient design of IRS-NOMA networks," *IEEE Trans. Veh. Technol.*, vol. 69, no. 11, pp. 14088–14092, Nov. 2020.

[34] S. Basharat et al., "Intelligent radio resource management in reconfigurable IRS-enabled NOMA networks," *Phys. Commun.*, vol. 53, Aug. 2022, Art. no. 101744.

[35] W. Song, S. Rajak, S. Dang, R. Liu, J. Li, and S. Chinnadurai, "Deep learning enabled IRS for 6G intelligent transportation systems: A comprehensive study," *IEEE Trans. Intell. Transp. Syst.*, vol. 24, no. 11, pp. 12973–12990, Nov. 2023.

[36] Q. Mao, F. Hu, and Q. Hao, "Deep learning for intelligent wireless networks: A comprehensive survey," *IEEE Commun. Surveys Tuts.*, vol. 20, no. 4, pp. 2595–2621, 4th Quart., 2018.
[37] H. Huang et al., "Deep learning for physical-layer 5G wireless techniques: Opportunities, challenges and solutions," *IEEE Wireless Commun.*, vol. 27, no. 1, pp. 214–222, Aug. 2020.
[38] Narengerile and J. Thompson, "Deep learning for signal detection in non-orthogonal multiple access wireless systems," in *Proc. UK/ China Emerg. Technol. (UCET)*, 2019, pp. 1–4.
[39] A. Emir, F. Kara, H. Kaya, and X. Li, "Deep learning-based flexible joint channel estimation and signal detection of multi-user OFDM-NOMA," *Phys. Commun.*, vol. 48, Oct. 2021, Art. no. 101443.
[40] P. Zhu, X. Wang, X. Jia, and Y. Xu, "Deep learning-based signal detection with soft information for MISO-NOMA systems," in *Proc. 94th Veh. Technol. Conf. (VTC)*, 2021, pp. 1–5.
[41] A. Emir, F. Kara, H. Kaya, and H. Yanikomeroglu, "DeepMuD: Multi-user detection for uplink grant-free NOMA IoT networks via deep learning," *IEEE Wireless Commun. Lett.*, vol. 10, no. 5, pp. 1133–1137, May 2021.
[42] K. Chitti, J. Vieira, and B. Makki, "Deep-learning based multiuser detection for NOMA," 2020, *arXiv:2011.11752*.
[43] G. Gui, H. Huang, Y. Song, and H. Sari, "Deep learning for an effective nonorthogonal multiple access scheme," *IEEE Trans. Veh. Technol.*, vol. 67, no. 9, pp. 8440–8450, Sep. 2018.
[44] Y. Xie, K. C. Teh, and A. C. Kot, "Deep learning-based joint detection for OFDM-NOMA scheme," *IEEE Commun. Lett.*, vol. 25, no. 8, pp. 2609–2613, Aug. 2021.
[45] C. Nguyen, T. M. Hoang, and A. A. Cheema, "Channel estimation using CNN-LSTM in RIS-NOMA assisted 6G network," *IEEE Trans. Mach. Learn. Commun. Netw.*, vol. 1, pp. 43–60, May 2023, doi: 10.1109/TMLCN.2023.3278232.
[46] D. V. Ratnam and K. N. Rao, "Bi-LSTM based deep learning method for 5G signal detection and channel estimation," *AIMS Electron. Elect. Eng.*, vol. 5, no. 4, pp. 334–341, 2021.
[47] A. Taha, M. Alrabeiah, and A. Alkhateeb, "Enabling large intelligent surfaces with compressive sensing and deep learning," *IEEE Access*, vol. 9, pp. 44304–44321, 2021.
[48] F. Jiang, L. Yang, D. B. da Costa, and Q. Wu, "Channel estimation via direct calculation and deep learning for RIS-aided mmWave systems," 2020, *arXiv:2008.04704*.
[49] T.-H. Vu, T.-V. Nguyen, D. B. Da Costa, and S. Kim, "Reconfigurable intelligent surface-aided cognitive NOMA networks: Performance analysis and deep learning evaluation," *IEEE Trans. Wireless Commun.*, vol. 21, no. 12, pp. 10662–10677, Dec. 2022.
[50] L. Tong and Q. Zhao, "Joint order detection and blind channel estimation by least squares smoothing," *IEEE Trans. Signal Process.*, vol. 47, no. 9, pp. 2345–2355, Sep. 1999.
[51] M. Biguesh and A. B. Gershman, "Training-based MIMO channel estimation: A study of estimator tradeoffs and optimal training signals," *IEEE Trans. Signal Process.*, vol. 54, no. 3, pp. 884–893, Mar. 2006.

HALEEMA SADIA received the B.Sc. degree in telecommunication engineering from the University of Engineering and Technology, Taxila, Pakistan, in 2015, the M.S. degree in electrical engineering from the NUST College of Electrical and Mechanical Engineering, Pakistan, in 2018, and the Ph.D. degree in electrical engineering from the Ghulam Ishaq Khan Institute of Engineering Sciences and Technology, Pakistan, in 2024, where she was a Graduate Research Assistant from 2021 to 2024. She worked as a Research Assistant with HITEC University Taxila, Pakistan, from 2015 to 2016. She also served as an IT Instructor for USF from 2018 to 2021. She is currently a Postdoctoral Research Fellow with the Department of Electrical and Communication Engineering, College of Engineering, United Arab Emirates University, Al Ain, UAE. Her research areas include wireless communication networks, NOMA for 5G networks, multi-user MIMO systems, intelligent reflecting surfaces, optimization techniques for B5G networks, and ML for 5G and B5G wireless networks.

HAFSA IQBAL (Member, IEEE) received the International Joint Doctorate degree (cum laude) from the University of Genoa, Italy, and the Carlos III University of Madrid, Spain, in 2022, where she is currently a Postdoctoral Researcher with Autonomous Mobility and Perception Lab and actively involved in the EU project on Ecomobility and Safe Perception. From 2022 to 2024, she served as an Assistant Professor with the National University of Sciences and Technology, Pakistan, where she was a member of the AI and Autonomous Systems Group. Her research focuses on computer vision, machine learning, and deep learning techniques for cognitive and interactive environments. During her M.S. degree, she was awarded the President's Gold Medal in 2022.

SYED FAWAD HUSSAIN (Senior Member, IEEE) received the M.S. degree in computer science from the Pierre and Marie Curie University (currently Paris-Sorbonne University), Paris, France, and the Ph.D. degree in computer science from the University of Grenoble (currently Grenoble Alpes University), Grenoble, France. He is currently an Associate Professor of computer science with the University of Birmingham, Dubai. Prior to joining the University of Birmingham, he has been associated with GIK Institute, Topi, where he worked as a Faculty Member for 11 years and as dean of graduate studies for one year. He has been involved in curriculum development at the university and national level as co-chair of the national curriculum revision committee at the Higher Education Commission, Pakistan. He is also working in multiple application domains including social media analysis, classifying ECG/EEG signals for mobile healthcare, and other interdisciplinary areas. His research interests include developing supervised and unsupervised learning algorithms for high-dimensional data, co-clustering and multi-view clustering, and semantic kernels.

NASIR SAEED (Senior Member, IEEE) received the B.Sc. degree in telecommunication from the University of Engineering and Technology, Peshawar, Pakistan, in 2009, the M.Sc. degree in satellite navigation from Politecnico di Torino, Italy, in 2012, and the Ph.D. degree in electronics and communication engineering from Hanyang University, Seoul, South Korea, in 2015. He was an Assistant Professor with the Department of Electrical Engineering, IQRA National University, Peshawar, from 2015 to 2017. From July 2017 to December 2020, he was a Postdoctoral Research Fellow with the Communication Theory Laboratory, King Abdullah University of Science and Technology. He is currently an Associate Professor with the Department of Electrical and Communication Engineering, United Arab Emirates University, Al Ain, UAE. He has published more than 80 international journal and conference articles. His research interests include non-conventional communication networks, heterogeneous vertical networks, multi-dimensional signal processing, and localization. He is an Associate Editor of IEEE WIRELESS COMMUNICATIONS LETTERS.